Applied Surface Science 255 (2009) 8539–8543

Contents lists available at ScienceDirect

Applied Surface Science

journal homepage: www.elsevier.com/locate/apsusc

Reactivity of lithium exposed graphite surface

S.S. Harilal [a,*], J.P. Allain [a], A. Hassanein [a], M.R. Hendricks [b], M. Nieto-Perez [c]

[a] Purdue University, School of Nuclear Engineering, 400 Central Dr., West Lafayette, IN 47907, USA
[b] Argonne National Laboratory, 9700 S. Cass Avenue, Argonne, IL 60439, USA
[c] CICATA-IPN, Cerro Blanco 141 Cimatario, Queretaro QRO 76090, Mexico

ARTICLE INFO

Article history:
Received 31 January 2009
Received in revised form 1 June 2009
Accepted 4 June 2009
Available online 11 June 2009

Keywords:
Plasma-facing components
X-ray photoelectron spectroscopy
Low-energy ion scattering spectroscopy
Lithium
Lithium–graphite intercalation

ABSTRACT

Lithium as a plasma-facing component has many attractive features in fusion devices. We investigated chemical properties of the lithiated graphite surfaces during deposition using X-ray photoelectron spectroscopy and low-energy ion scattering spectroscopy. In this study we try to address some of the known issues during lithium deposition, viz., the chemical state of lithium on graphite substrate, oxide layer formation mechanisms, Li passivation effects over time, and chemical change during exposure of the sample to ambient air. X-ray photoelectron studies indicate changes in the chemical composition with various thickness of lithium on graphite during deposition. An oxide layer formation is noticed during lithium deposition even though all the experiments were performed in ultrahigh vacuum. The metal oxide is immediately transformed into carbonate when the deposited sample is exposed to air.

1. Introduction

Wall conditioning is essential for obtaining less erosion and high performance plasma confinement in fusion devices [1–5]. For example, wall conditioning with thin lithium layers gives rise to low hydrogen recycling and reduction in oxygen and carbon impurities [2,6]. In the National Spherical Torus Experiment (NSTX) magnetic fusion device, a lithium coating was introduced on graphite tiles and produced significant improvements in plasma conditions although the underlying physics is an issue [2,7–9]. Apart from applications in fusion devices, lithium–graphite intercalation compounds (LGIC) have been extensively used in lithium ion batteries and presently many groups are working to improve the energy storage capabilities [10–16].

It is well known that lithium atoms intercalate into the bulk graphite when it is deposited on a graphite substrate [17–19]. The investigation of lithium–graphite intercalation is essential to understand some of the known lithium conditioning effects in tokamaks [5]. In spite of numerous researches in this field, the presence of Li on the first wall sometimes yielded contrary results with different fusion devices and hence numerous questions exist regarding the interaction of Li with graphite and interaction of plasma species with lithiated graphite [20]. It is reported that the lithium conditioning suppresses both physical and chemical sputtering of graphite [21,22]. Most of the lithium conditioning effects including hydrogen retention and impurity suppression are expected to be directly proportional to the concentration of lithium on the surface [18]. Hence the effect of lithium on plasma–wall interactions is expected to depend on the concentration as well chemical state of lithium near the surface of the plasma-facing components.

Although extensive research has been carried out with lithium in the solid and liquid states [3,6,7,20,21,23–29], understanding the behavior of lithium on graphite surfaces is limited. Hence the objective of this study is directed to understand the state of lithium and its reactivity during the deposition of lithium on a ATJ graphite substrate. We studied the chemical properties of 'as received' NSTX ATJ graphite tiles and noticed strong presence of lithium carbonate. The exposure of 'as received' NSTX tiles to air for prolonged time (~3 months) can initiate chemical reactions in deposited lithium. Lithium is a highly reactive element and oxidizes very easily and hence it is essential to simulate an experimental environment to evaluate lithium doping and its time-dependent chemical state variation. We carried out X-ray photoelectron spectroscopic analysis during deposition of lithium on an ATJ graphite substrate and investigated the changes in chemical state with various thicknesses of lithium. In this work we report some preliminary results of the chemical state of lithium on graphite substrate and its time dependent changes, oxide layer formation mechanisms and chemical change during exposure of the sample to ambient air.

2. Experimental

The Interaction of Materials with Particles and Components Testing (IMPACT) experimental facility has been designed to study

* Corresponding author. Tel.: +1 765 496 3852; fax: +1 765 496 2233.
E-mail address: sharilal@purdue.edu (S.S. Harilal).

0169-4332/$ – see front matter © 2009 Elsevier B.V. All rights reserved.
doi:10.1016/j.apsusc.2009.06.009

in situ dynamic heterogeneous surfaces at the nano-scale exposed to varied environments that modify surface and interface properties [30]. The IMPACT experiment achieves this by atomic-scale characterization of the evolution of elemental, chemical, and thermodynamic states of ultra-thin film surface and interfaces using complementary surface-sensitive characterization techniques. *In situ* techniques used in the IMPACT experiment include: low-energy ion scattering spectroscopy (LEISS) with simultaneous forward and backward scattering modes, direct recoil spectroscopy, X-ray and Auger photoelectron spectroscopy, and mass spectrometry using both quadrupole and magnetic sector analyzers.

The experimental details of the IMPACT facility can be found elsewhere [30]. The facility consists of an ultrahigh vacuum vessel and a vacuum of $\sim 10^{-9}$ Torr is routinely achieved. The sample is inserted in the chamber via a load–lock system. The chamber is equipped with various ion and electron guns, thermal e-beam evaporation source, X-ray and EUV photon sources. The detection tools include a hemispherical energy analyzer, a quartz crystal microbalance dual-crystal unit (QCM-DCU), mass spectrometers etc. XPS measurements are performed using non-monochromatic Mg Kα X-ray source at 1253.6 eV. The emitted core electrons are analyzed using a hemispherical energy analyzer (Phoibos 100, Specs), which is equipped with a 5-channel electron multiplier detector. The core peaks were recorded with a pass-energy of 15 eV. The resolution of the XPS diagnostics system is 0.8 eV.

For performing LEISS, a 2 keV He^+ source is used in the forward scattering mode to detect Li on the graphite matrix and the forward scattered ions were collected using the same detector used for XPS. The angle of incidence for the ion beam with respect to the sample surface normal was set at 65°. More details about the LEISS and XPS have been given in a recent publication [30].

For Li deposition, a four-pocket electron beam evaporator EGN-4 from Oxford Applied Research was used. The evaporator has also been custom designed to operate facing downward, which is particularly difficult for low-melting metals such as Sn and Li. An effusion cell was used for loading lithium onto the evaporator crucible. For avoiding oxidation of lithium, loading of the lithium filled crucible in the evaporator is done with minimum time in air. The *in situ* calibration of deposition rate was done using a quartz crystal microbalance (QCM) and details of the calibration procedure can be found elsewhere [30]. The electron-beam evaporator is equipped with an *in situ* current monitor for closed-loop operation regulating the particle current from the evaporator. This is accomplished by sampling a small fraction of the vapor, which is intrinsically in an ionized state. Once the current is set, the mass gain of the crystal is monitored until a constant slope in the crystal frequency is established. This step is repeated for different current values and a plot of the QCM frequency slope vs evaporator current is generated. Conversion of the frequency slope to deposition rate is conducted using Sauerbrey equation [30]. ATJ graphite [31] samples are prepared by cutting 3 mm thick disks from a 1 cm diameter rod. Samples are polished and cleaned by Ar sputtering in vacuo.

Lithium has high reactivity towards oxygen and it requires special attention in the laboratory experiments. Deposition of Li is done using a lithium evaporator with a controlled rate of 1 nm/min at room temperature. Due to constrains of the lithium evaporator, the maximum thickness of lithium deposition is limited to ~150 nm. All *in situ* analysis were carried out with a chamber base pressure $\sim 10^{-9}$ Torr. The measured water content in the chamber using a residual mass spectrometer is less than 10^{-10} Torr.

3. Results and discussion

We analyzed the chemical state of 'as received' lithium exposed boronated ATJ graphite NSTX tiles using X-ray photoelectron spectroscopy. Typical XPS spectrum of a NSTX tile is given in Fig. 1. The XPS spectrum clearly shows the core peaks due to C, O, B, Li. The spectrum also shows the presence of satellite peaks at slightly higher binding energies with respect to core peaks arising due to non-monochromaticity of the X-ray source. We noticed strong presence of Li_2CO_3 peak at 290.2 eV [32]. It should be mentioned the fact that the air exposed 'as received' tiles may contain a film of water, oxygen, hydrocarbon, carbon oxides etc. and these adsorbents can interact with Li, which may lead to formation of carbonate compounds. Many of the previous studies suggested the chemical state of lithium changes dynamically and the ambient conditions strongly affect the morphology of deposited lithium [33]. A study of reactivity of Li on graphite will be useful to address several issues related Li deposited graphite tiles in NSTX including lifetime of lithium layer on the substrate surface, state of Li during deposition, oxide and carbonate layer formation over deposited lithium.

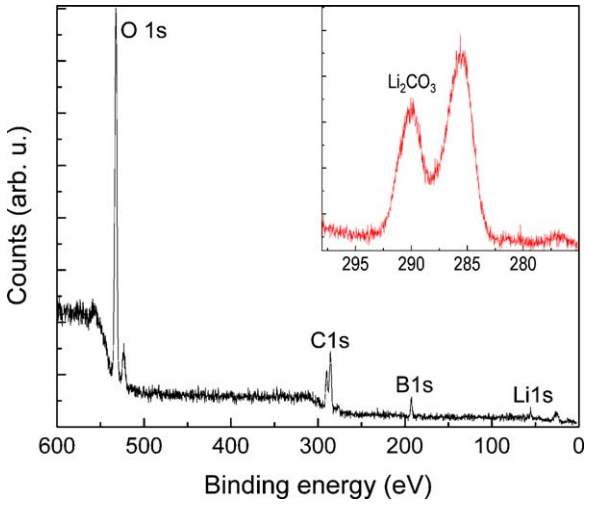

Fig. 1. XPS core electron spectra obtained from a NSTX tile. These are ATJ boronated and lithium deposited graphite tile. Various core electron lines are identified in the figure. Inset shows the C 1s line indicating the presence of lithium carbonate.

We simulated the deposition conditions at NSTX using the IMPACT facility. ATJ graphite surface is selected as the substrate for lithium deposition. Before depositing Li, the polished graphite substrate is ion cleaned to remove any adsorbent attached to the surface. XPS measurements were made during deposition at various intervals. XPS line shape analysis provides qualitative information and identification of changes in the chemical state of atoms and complex molecule and hence it is a versatile tool for *in situ* surface analysis. The *in situ* XPS spectra obtained for C 1s and O 1s are given in Fig. 2 along with representative fitted peaks for various Li deposition conditions on ATJ graphite. All XPS measurements were done immediately after deposition of lithium with different thicknesses. The total thickness of the deposited lithium on graphite is 140 nm. Also the 140 nm lithium deposition on the substrate is not made continuously instead, deposition is halted at various intervals in order to analyze the sample using XPS. The XPS signal obtained from the pristine graphite is also given in Fig. 2 for reference. For curve fitting of the data, Gaussian profiles have been used. C 1s XPS core peak observed at 284.6 eV with an asymmetric shape is assigned to graphitic peak. The high reactivity of Li induced changes in the composition of the surface films which can be understood with photoelectron spectra of C 1s, and O 1s. With lithium addition, the C 1s peak becomes more asymmetric indicating the presence of second component possibly due to C–O bond. There is no clear evidence for the formation of lithium carbonate (Li_2CO_3, 290.2 eV) in the C 1s core spectrum. The O 1s photoelectron peak showed dramatic variation with Li doping

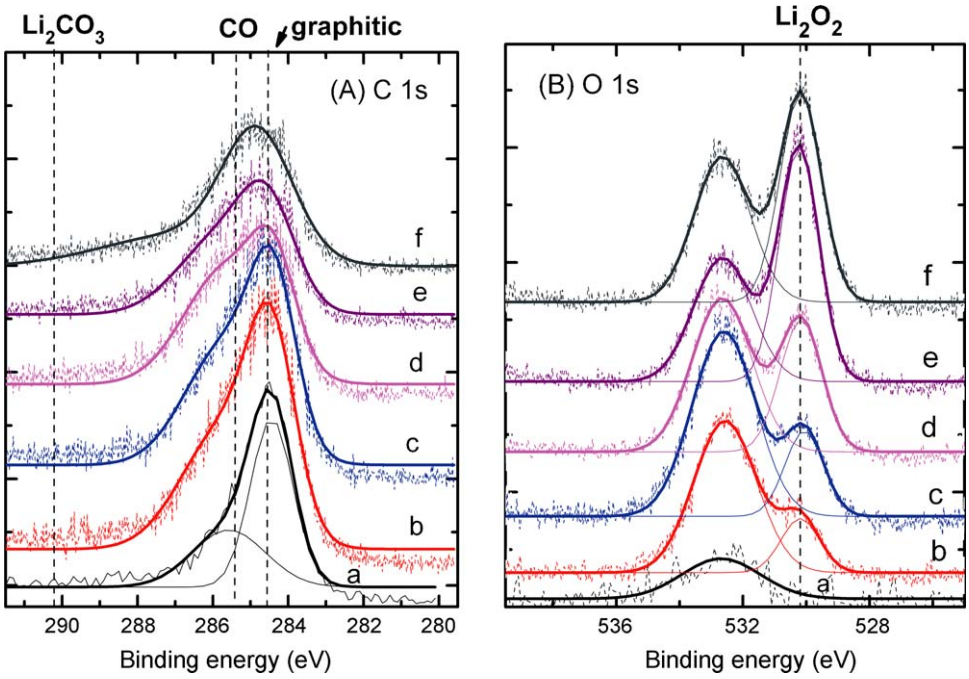

Fig. 2. XPS spectra of various core photoelectron lines with varying lithium thickness on graphite substrate for (A) C 1s and (B) O 1s photoelectron lines. The core electron spectrum obtained from (a) pristine graphite substrate is also shown along with various lithium thickness on graphite surface (b) 30 nm; (c) 45 nm; (d) 60 nm; (e) 120 nm and (f) 140 nm.

with changes in peak shape. With lithium deposition a new peak at 530.2 eV is observed and its intensity increased with increase in Li thickness (shown in Fig. 2B).

A new binding energy peak at 530.2 eV is formed during Li addition. The origin of this new peak can be due to oxidation of Li with impurity oxygen present in the chamber. As mentioned earlier, the chamber contains a water content of $\sim 10^{-10}$ Torr. Also oxidation of the lithium can be happened during evaporator loading. So during deposition, these oxygen contaminants can react with Li, which may lead to the formation of lithium oxides and peroxides (Li_2O, Li_2O_2) and other radicals containing lithium and oxygen (Li_2CO_3, LiOH). Towe et al. [33] observed similar O 1s binding energy peak around 530.2 eV during lithium deposition on a amorphous carbon substrate and a mild treatment of oxygen and assigned the peak due to metal oxide formation. The reported peak location for Li_2O in the literature is 528.8 eV [34–37]. We believe

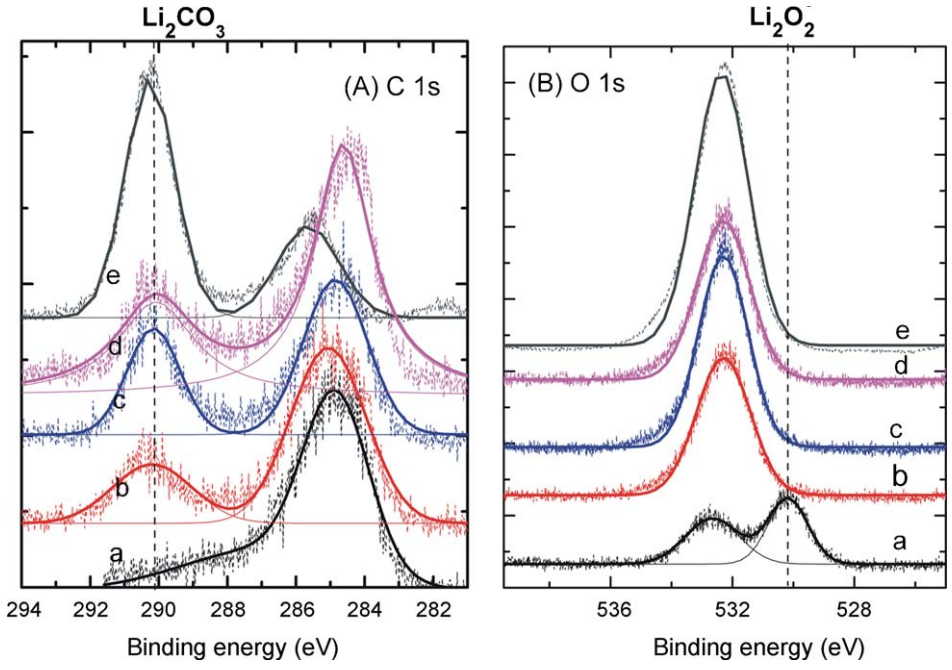

Fig. 3. Core photoelectron spectra obtained from Li deposited graphite target with various duration of air exposure is shown for (A) C 1s and (B) O 1s photoelectron peaks. For comparison the XPS spectral details of Li deposited sample without air exposure (a) and XPS spectrum from NSTX tile (e) is also given. The air exposure durations are (b) 1 h (c) 24 h and (d) 7 days.

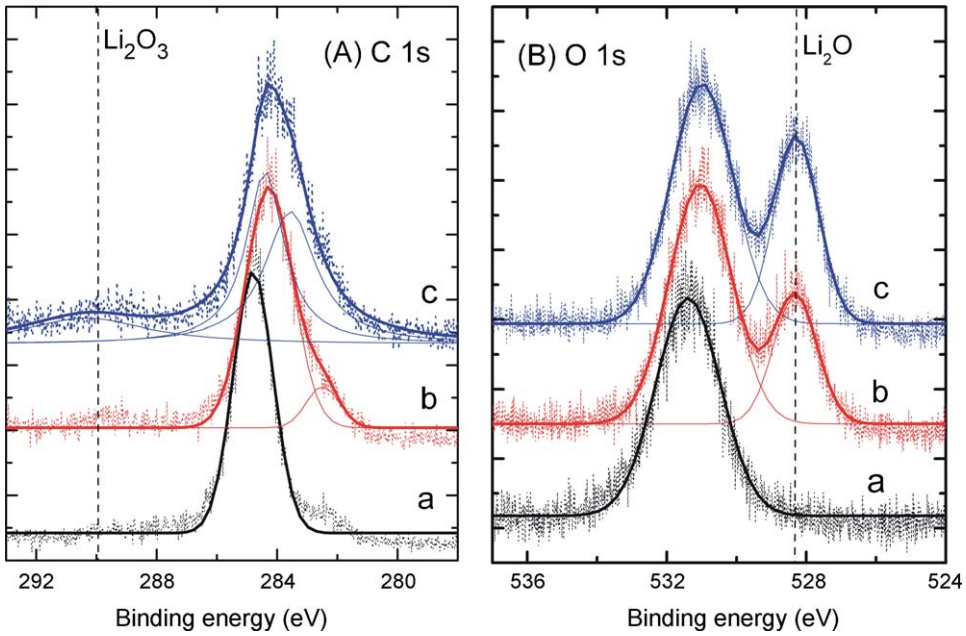

Fig. 4. (A) C 1s and (B) O 1s photoelectron spectra obtained from 'as received' Li metal sample is given in (a). Photoelectron spectra obtained from the Li sample after 20 mts (b) and 40 mts (c) of 2 keV Ne^+ cleaning is also given.

the peak observed at 530.2 eV is due to the presence of Li_2O_2 [36], The assignment of O 1s peak around 533 eV can be considered to be sub-oxides and hydroxides, un-reacted adsorbed oxide etc [33]. The reported binding energy of LiOH is 531.6 eV [34]. The presence of residual water in the chamber is involved in the formation of hydroxide radicals. Also the presence of lithium carbonate is unlikely by examining the C 1s spectra.

The XPS analysis of NSTX tiles showed strong presence of Li_2CO_3 and it is not evidenced in our *in situ* analysis of lithium deposition on ATJ graphite. It is likely that the exposure of NSTX tiles to air may affect the surface composition by reaction with oxygen. To confirm our hypothesis, we exposed the lithium deposited sample to air for certain periods with subsequent XPS analysis. The XPS spectra obtained with air-exposed samples are given in Fig. 3 along with fitted curves for C 1s and O 1s. For comparison, the XPS spectra obtained from the NSTX tile is also given. After exposing the sample to air, the most interesting feature is observed for C 1s and O 1s core spectra. In the C 1s spectra, a new peak is observed at 290.2 eV [34] and it is assigned to Li_2CO_3 and its intensity increased with duration of air exposure from 1 to 24 h. In the O 1s peak, the most interesting feature is the disappearance of the peak at 530.2 eV even after exposing the sample to air for one hour. This leads to the conclusion that the formation of Li_2CO_3 is linked with the disappearance of peroxide peak observed at 530.2 eV. The carbonate compound could be formed by the interaction of peroxide lithium compounds with CO_2 or CO during the exposure of the lithium deposited sample with air.

The XPS analysis of Li deposited ATJ graphite showed the presence of peroxide functionality and during the air exposure the lithium peroxide is transformed into carbonate functionality. The oxidation of the lithium during deposition can be related to presence of oxygen in the chamber as an impurity. All *in situ* deposition experiments were carried out in ultra high vacuum. The other source of oxidation is from the contaminated lithium in the evaporator. In order to get more information about the oxidation behavior of lithium, XPS analysis has been performed with pure 'as received' lithium metal sample. To avoid any contamination to the lithium sample during the loading of the sample into UHV chamber, the sample was removed from the packing in an argon environment in the load–lock and placed on the sample holder. XPS analysis of the lithium sample showed strong charging effects and the obtained photoelectron spectra are calibrated using the CH impurity line observed at 284.8 eV. These charging effects are induced by the presence of insulating species at the surface of the sample and are well documented in literature [38].

XPS spectra obtained from metal lithium is given in Fig. 4 along with fitted peaks for C 1s and O 1s core electron peaks. The C 1s core line corresponding to CH peaked at 284.8 is used for calibration. The carbonate functionality is found to be absent in the 'as received' lithium metal and with the use of 2 keV Ne^+ beam cleaning a weak presence of Li_2CO_3 appeared at 290.2 eV. For the 'as received' lithium metal the O 1s core peaked at 531.5 eV. After 2 keV ion cleaning a new peak is formed in the O 1s core spectra at 528.6 eV and its intensity is found to increase with increasing time of ion etching. This peak is assigned to Li_2O [34]. The O 1s core peak at 531.5 eV indicates the presence of hydroxide and carbonate radicals. But comparing with C 1s core peak spectra, the main radicals could be hydroxide as the carbonate functionality is found to be weak in the C 1s spectra. By considering all spectra obtained with the lithium metal sample, one can conclude that the metal target is covered by a film of hydroxide on the top surface followed by lithium oxide layer which is consistent with previous observation [39].

The carbonate functionality is evident in the air exposed lithium deposited graphite. The Li_2CO_3 photoelectron peak intensity is enhanced when the air exposure time increased from 1 to 24 h and its intensity is slightly reduced when the sample is kept in air for 7 days. By comparison, the core spectra obtained from NSTX tiles indicated that carbonate function is much stronger than that observed with air exposed lithium deposited sample even though these tiles were kept in air for longer time (more than 2 months). One reason for this disparity may come from the fact that the deposited lithium thickness in NSTX tiles are much higher (2–5 μm) compared to 140 nm lithium deposition in the present case.

The formation channel of the carbonate functionality in the presence of air can be linked with lithium peroxide as the peroxide functionality disappears when the sample is exposed to air. It is well known that lithium peroxide can be used as a non-

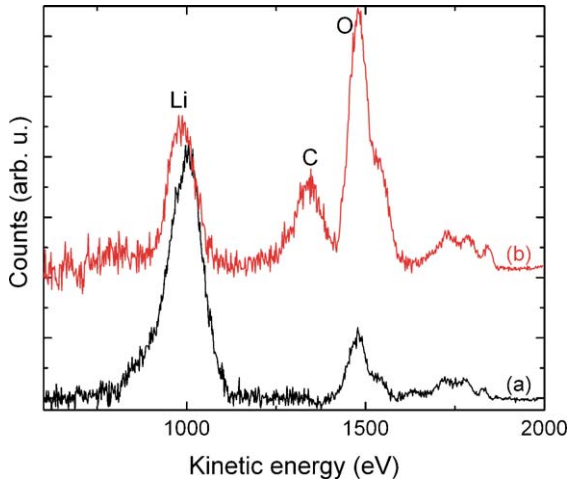

Fig. 5. LEISS scans of lithiated graphite surface. (a) LEISS spectra taken immediately after lithium deposition is given and (b) LEISS scan taken after keeping the lithium deposited sample in UHV for 24 h.

regenerative air revitalization material for oxygen supply and carbon dioxide removal. When exposed to air, lithium peroxide may interact with ambient carbon dioxide which leads to lithium carbonate formation ($2Li_2O_2 + 2CO_2 \rightarrow 2Li_2CO_3 + O_2$).

It is reported that graphite intercalates lithium atoms in its hexagonal layer planes and the rapid diffusion of lithium leads to dramatic reduction of physical and chemical sputtering of graphite [19,21]. *In situ* XPS provided the chemical state information of probing depths from 2–3 monolayers down to about 10–15 monolayers into the deposited material. So it is imperative to understand the state of Li during deposition on the top of the surface (first few monolayers) and LEISS is one of the few real-space techniques able to probe the first and second monolayer of a surface. LEISS analysis was performed with a 2 keV He^+ beam. Typical background corrected LEISS spectra recorded just after lithium deposition and 24 hrs later (by keeping the deposited sample in the UHV chamber) are given in Fig. 5. The assignment of various peaks observed in the LEISS spectra is also given in figure. The shifts noticed in the peaks are lower than 10% in energy predicted by elastic collision theory. The shifts are due to inelastic energy losses during the scattering event and variation in the angle between the beam and the detector [30]. It is very clear from the LEISS spectra that Li peak is found to be very intense just after the deposition while, carbon peak at 1346 eV is almost absent. But the LEISS spectra taken with the same sample after 24 h showed (by keeping the deposited sample in UHV) presence of carbon on the top layer with reduced atomic fraction of lithium. The atomic fraction measurement with LEISS showed the lithium and oxygen fractions occupy 96.6% and 3.4% respectively on the first few monolayers just after lithium deposition and the estimated atomic fraction corresponding to LEISS taken after 24 h gives 66%, 11% and 23% of lithium, carbon and oxygen respectively. It indicates oxidation of lithium happening during deposition. The source of oxygen can be due to water and oxygen impurities in the chamber and/or oxygen impurity from the evaporator. The presence of carbon on the top monolayers after keeping the sample for 24 h clearly indicates that lithium diffused into the sample and intercalated with graphite.

4. Conclusion

In situ surface chemistry analyses have been carried out on a lithiated graphite surface during lithium deposition. The surface-sensitive diagnostic tools used are X-ray photoelectron spectroscopy and ion scattering spectroscopy. XPS studies during lithium deposition showed changes in the composition and electronic structure with various concentrations of lithium on graphite. During the deposition, the doped lithium is found to interact strongly with various impurities in the chamber. A lithium peroxide peak is observed during lithium deposition on the ATJ graphite substrate. The carbonate radicals appeared at the expense of peroxide functionality when the sample was exposed to air for a short time (one hour). It shows the metal oxide immediately transformed into carbonate when the deposited sample is exposed to air. The XPS data obtained with air exposed samples are consistent with data obtained with NSTX tiles where carbonate radicals are very strong and oxide radicals are not evident. XPS studies of pure lithium targets showed a film of hydroxide on the top surface followed by lithium oxide layer and absence of peroxide functionality. It shows the lithium peroxide formation is influenced by the graphite substrate. LEISS studies indicate lithium diffuse into the sample and intercalate with graphite.

References

[1] J. Winter, Fusion Technol. 29 (1996) 278.
[2] D.K. Mansfield, D.W. Johnson, B. Grek, H.W. Kugel, M.G. Bell, R.E. Bell, R.V. Budny, C.E. Bush, E.D. Fredrickson, K.W. Hill, D.L. Jassby, R.J. Maqueda, H.K. Park, A.T. Ramsey, E.J. Synakowski, G. Taylor, G.A. Wurden, Nucl. Fusion 41 (2001) 1823.
[3] R. Kaita, R. Majeski, R. Doerner, T. Gray, H. Kugel, T. Lynch, R. Maingi, D. Mansfield, V. Soukhanovskii, J. Spaleta, J. Timberlake, L. Zakharov, J. Nucl. Mater. 363–365 (2007) 1231.
[4] R.J. Hawryluk, Rev. Mod. Phys. 70 (1998) 537.
[5] D. Stotler, T. Rognlien, S.I. Krasheninnikov, Phys. Plasmas 15 (2008) 058303.
[6] S.V. Mirnov, V.B. Lazarev, S.M. Sotnikov, V.A. Evtikhin, I.E. Lyublinski, A.V. Vertkov, Fusion Eng. Des. 65 (2003) 455.
[7] H.W. Kugel, M.G. Bell, R. Bell, C. Bush, D. Gates, T. Gray, R. Kaita, B. Leblanc, R. Maingi, R. Majeski, D. Mansfield, D. Mueller, S. Paul, R. Raman, A.L. Roquemore, S. Sabbagh, C.H. Skinner, V. Soukhanovskii, T. Stevenson, L. Zakharov, J. Nucl. Mater. 363 (2007) 791.
[8] J.E. Menard, et al. Nucl. Fusion 47 (2007) S645.
[9] M. Ono, et. al, Plas. Phys. Contr. Fusion 45 (2003) A335.
[10] R. Alcantara, P. Lavela, J.L. Tirado, E. Zhecheva, R. Stoyaneva, J. Solid State Electrochem. 3 (1999) 121.
[11] C. Lee, B. Mun, P.N. Ross Jr., J. Electrochem. Soc. 149 (2002) A1286.
[12] J.M. Tarascon, D. Guyomard, Electrochim. Acta 38 (1993) 1221.
[13] Q.H. Wu, A. Thissen, W. Jaegermann, Appl. Surf. Sci. 250 (2005) 57.
[14] K. Xu, Chem. Rev. 104 (2004) 4303.
[15] G. Zhuang, Y. Chen, P.N. Ross Jr., Surf. Sci. 418 (1998) 139.
[16] D. Ensling, A. Thissen, W. Jaegermann, Appl. Surf. Sci. 255 (2008) 2517.
[17] C.M. Lee, S.-H. Yang, B.-J. Mun, P.N. Ross Jr., Surf. Sci. 477 (2001) 126.
[18] N. Itou, H. Toyoda, K. Morita, H. Sugai, J. Nucl. Mater. 290 (2001) 281.
[19] J.R. Dahn, T. Zheng, Y. Liu, J.S. Xue, Science 270 (1995) 590.
[20] M.Z. Racic, D. Ruzic, D. Raju, C. Struck, C.H. Castano, 22nd IEEE Symposium on Fusion Engineering, Albuquerque, NM, (2007), 323.
[21] H. Yagi, H. Toyoda, H. Sugai, J. Nucl. Mater. 313 (2003) 284.
[22] J.P. Allain, D. Rokusek, S.S. Harilal, M. Nieto, C.H. Skinner, H. Kugel, B. Heim, R. Kaita, R. Majeski, J. Nucl. Mater. 390–91 (2009) 942.
[23] J.P. Allain, D.G. Whyte, J.N. Brooks, Nucl. Fusion 44/5 (2004) 655.
[24] J.P. Allain, D.N. Ruzic, M.R. Hendricks, J. Nucl. Mater. 290 (2001) 180.
[25] J.P. Allain, D.N. Ruzic, D.A. Alman, M.D. Coventry, Nucl. Instrum. Methods Phys. Res. B 239 (2005) 347.
[26] R.P. Doerner, M.J. Baldwin, S.I. Krasheninnikov, D.G. Whyte, J. Nucl. Mater. 313–316 (2003) 383.
[27] A. Hassanein, J.P. Allain, Z. Insepov, I. Konkashbaev, Fusion Sci. Technol. 47 (2005) 686.
[28] J.N. Brooks, J.P. Allain, T.D. Rognlien, R. Maingi, J. Nucl. Mater. 337–39 (2005) 1053.
[29] M. Narula, A. Ying, N.B. Morley, M. Ni, M.A. Abdou, 21st IEEE Symposium on Fusion Engineering, Knoxville, TN (2006) 251.
[30] J.P. Allain, M. Nieto, M.R. Hendricks, S.S. Harilal, A. Hassanein, Rev. Sci. Instrum. 78 (2007) 113105.
[31] ATJ is the trade name of Union Carbide graphite.
[32] NIST Standard Reference Database (www.nist.gov).
[33] M. Towe, P. Reinke, P. Oelhafen, J. Nucl. Mater. 290 (2001) 153.
[34] K. Kanamura, S. Shiraishi, H. Takezawa, Z. Takehara, Chem. Mater. 9 (1997) 1797.
[35] S. Tanaka, M. Taniguchi, H. Tanigawa, J. Nucl. Mater. 283–287 (2000) 1405.
[36] M.V. Landau, A. Gutman, M. Herskowitz, R. Shuker, Y. Bitton, D. Mogilyansky, J. Mol. Catal. A: Chem. 176 (2001) 127.
[37] I. Ismail, A. Noda, A. Nishimoto, M. Watanabe, Electrochim. Acta 46 (2001) 1595.
[38] A. Cros, J. Electron Spectrosc. Relat. Phenom. 59 (1992) 1.
[39] K. Kanamura, H. Tamura, S. Shiraishi, Z. Takehara, J. Electrochem. Soc. 142 (1995) 340.